coatings

MDPI

Article

Modified Epoxy with Chitosan Triazine Dihydrazide Derivatives for Mechanical and Corrosion Protection of Steel

Ayman M. Atta [1,*], Ayman El-Faham [1,2], Hamad A. Al-Lohedan [1] and Abdelrahman O. Ezzat [1]

[1] Department of Chemistry, College of Science, King Saud University, Riyadh 11451, Saudi Arabia; aelfaham@ksu.edu.sa (A.E.-F.); hlohedan@ksu.edu.sa (H.A.A.-L.); ao_ezzat@yahoo.com (A.O.E.)

[2] Chemistry Department, Faculty of Science, Alexandria University, P.O. Box 426, Ibrahimia, Alexandria 12321, Egypt

* Correspondence: atta@ksu.edu.sa

Received: 20 November 2020; Accepted: 17 December 2020; Published: 18 December 2020

Abstract: Modification of the curing exothermic reaction of epoxy resin with polyamine (PA) hardeners by new chemically bonded fillers to improve the mechanical properties and anticorrosion performances of the epoxy coatings is the main goal for wide applications of epoxy coatings. In this work, the chemical structure of chitosan was modified with triazine hydrazide moiety that contains primary, secondary, and tertiary amine groups to act as activator and dangling chain linkers during the curing of epoxy/PA system. Different molecular masses of chitosan were modified with triazine dihydrazide moiety (Ch-TH2), and their chemical structures and surface morphologies were identified. Their thermal stabilities were investigated, and the grafting percentages with triazine hydrazide were determined from thermal analysis. Different weight percentages of Ch-TH2 ranged from 1 to 10 Wt. % were added to the epoxy/PA system, and their curing characteristics, such as heat enthalpy and glass transition temperature, were determined from non-isothermal dynamic scanning calorimetric thermograms. The effects of molecular masses, triazine dihydrazide %, and Ch-TH2 Wt. % on the mechanical, adhesion and anticorrosive properties of the cured epoxy/PA coatings for steel were investigated. The optimum Ch-TH2 Wt. % was selected from 3 to 6 Wt. % to improve the mechanical, adhesion, and anticorrosive properties of the cured epoxy/PA coatings.

Keywords: epoxy coatings; chitosan; curing; salt spray; mechanical and adhesion; steel

1. Introduction

Naturally occurring chitosan biopolymers have been employed for different green applications to inhibit metal corrosion as binders, coatings, and corrosion inhibitors [1–3]. The presence of hydroxyl and amine groups in the chemical structure chitosan facilitates its capability to coordinate with the metal substrate at the metal/solution interfaces. The chemical modification of chitosan with new grafts and converting their molecular sizes from macro to nanocomposites were carried out to improve their metal protection applications [4–7]. The chemical linking of coating additives during the curing process of epoxy resin as a binder or curing agent attracted great attention, facilitating the improvement in the epoxy coating performances. These techniques were also used to improve their mechanical and anticorrosion properties as bio-based epoxy [8–10]. It is well known that petroleum-based polyamines have been widely used as curing agents for epoxy resin and classified as toxic materials. The polyamines adduct types sometimes were employed to reduce the toxicity [11]. It was previously reported that chitosan nanofibers were used to improve the thermal and mechanical properties of the epoxy resin cured with polyamines [10–13]. The development of eco-friendly epoxy and hardener based on

biopolymers is very important to produce green coatings. Therefore, it is interesting to investigate the effect of chitosan molecular masses and their grafting to form chitosan polyamines on the curing behaviors and coating performances of the epoxy coatings to protect the steel from corrosion in the aggressive marine environment.

Modification and blending of chitosan with different amines and Schiff base derivatives have been reported to be an effective technique to use as bio-polymeric protective coatings for the steel substrate [14–17]. Chitosan-polypyrrole composites have been loaded in epoxy coatings using the powder coating technique as superior inhibitive coatings for steel corrosion [14,15]. Novel triazole-modified chitosan was prepared by reaction of chitosan with 4-amino-5-methyl-1,2,4-triazole-3-thiol to form a protective layer for steel against corrosion in an acidic medium [16]. It was also reported that the loading of poly(aniline-anisidine)/chitosan/SiO_2 composite into epoxy coatings improved the coatings' performances of epoxy on the steel surfaces through chemical linking of chitosan composites with epoxy matrix [18]. The crosslinking of chitosan with genipin was also reported as an effective technique to improve the anticorrosion coatings of chitosan for different alloy substrates [19]. In this respect, the present work aims to modify the chemical structure of chitosan with 1,3,5-triazine 4,6-dihydrazide to increase their amine group contents. The chitosan grafts will apply to improve the curing characteristics of commercial epoxy resin with a polyamine hardener. The effect of chitosan molecular masses and grafts content on the curing, thermal, and mechanical properties of the cured epoxy films is another goal of the present study to produce non-cracked flexible epoxy coating films.

2. Experimental

2.1. Materials

All chemicals were delivered from Sigma–Aldrich Chemical Co. (St. Louis, MO, USA) and used to modify the chemical structure of chitosan. Chitosan (Ch) having different molecular masses low (LCh 50 KDa; viscosity 20 cP, 1 Wt. % in 1% acetic acid, and 89% degree of acetylation), medium (MCh 150 KDa; viscosity 300 cP, 1 Wt. % in 1% acetic acid and 84% degree of acetylation) and high (HCh 375 KDa; 2000 cP, 1 Wt. % in 1% acetic acid and 81% degree of acetylation) were used to investigate the effect of their molecular masses on their modification reactions. Cyanuric chloride (CC), hydrazine hydrate, trimethylamine $(CH_3CH_2)_3N$, acetonitrile, tetrahydrofuran (THF), acetic acid, and ethanol were used as chitosan modification reagents. Commercial Epikote epoxy resin 828 based on diglycidyl ether bisphenol A (DGEB) with epoxy equivalent weight 190–200 g/eq; Hexion, Olana, Italy) and its long chain length aliphatic polyamines Epikure™ 270 hardener (PA) were used to prepare epoxy coatings using the recommended weight ratio (4:1 Wt. %). Steel panels having the following chemical compositions: 0.14% C, 0.57% Mn, 0.21% P, 0.15%, 0.37% Si, 0.06% V, 0.03% Ni, 0.03% Cr and Fe balance were used as coating substrate.

2.2. Preparation of Chitosan Hydrazide (Ch-TH2)

Chitosan (LCh, MCh, or HCh 2.0 g) was suspended in THF (200 mL) under vigorous stirring at 5 °C. Cyanuric chloride (6.10 g; 100 mmol) and trimethylamine (100 mmol, 3.30 g) were slowly added to Ch suspension at temperature which ranged from 0 to 5 °C under vigorous stirring for 24 h. The solid was separated by filtration, washed with toluene, water, and ethanol, and then dried in a vacuum oven at 40 °C for 6 h. The solids were rinsed with methanol: THF (3:1) and dried at room temperature to afford the modified chitosan cyanuryl chloride Ch-TC2. The reaction yields of LCh-TC2, MCh-TC2, and HCh-TC2 were 92.5, 85.4, and 65.7%, respectively. The product of Ch-TC2 (10.0 g) was reacted with 20 mL of hydrazine hydrate (80%) in CH_3CN (60 mL), and the reaction mixture was refluxed for 6 h. The solid was then separated by filtration, washed with acetonitrile, ethanol, and then dried at 60 °C for 12 h. The chitosan 1,3,5-triazine 4,6-dihydrazide grafts (Ch-TH2) were abbreviated as LCh-TH2, MCh-TH2, and HCh-TH2.

2.3. Characterization of Ch-TH2 and Their Epoxy Composites

The chemical structure of Ch and Ch-TH2 was verified from Fourier transform infrared analysis (Nicolet Magna 750 FTIR spectrometer using KBr, Newport, NJ, USA) and hydrogen nuclear magnetic resonance (^{1}HNMR 400 MHz 400 MHz Bruker Avance DRX-400 spectrometer; Toronto, ON, Canada). The thermal stability of Ch and Ch-TH2 was evaluated using thermogravimetric analysis (TGA-NETZSCH STA 449 C instrument, New Castle, DE, USA) under an N_2 atmosphere with a heating rate of 10 °C min^{-1}. The surface morphologies of Ch and Ch-TH2 were evaluated by using scanning electron microscopy (JEOL JXA-840A, Tokyo, Japan) at operating voltage 5–10 kV.

2.4. Curing and Coatings of DGEB/PA/Ch-TH2 Composite

The curing exothermic peaks of DGEB/PA in the absence and presence of Ch-TH2 were evaluated using differential scanning calorimetry (DSC; Q10 DSC calorimeter from TA Instrument, New Castle, DE, USA) in non-isothermal dynamic mode at a heating rate 5 °C·min^{-1} from −30 to 300 °C. In this respect, the sample of DGEB/PA (5–7 mg) was sealed in aluminum cups, sealed, heated under N_2 purge of 50 mL·min^{-1}, and the empty cup was used as blank. The glass transition temperature (T_g) and the heat evolved during the reaction of the mixture (ΔH) were evaluated from two runs. The first run was carried out from −30 to 200 °C and the second run was from −30 to 300 °C. The exothermic heat flow of each cured sample was determined non-isothermal.

Ch-TH2 (LCh-TH2, MCh-TH2, or HCh-TH2) was added with different weight ratios ranged from 1 to 6 Wt. related to the total weight of DGEB/PA. In this respect, the specific selected weight of Ch-TH2 was dissolved in an aqueous acetic solution (2 Wt. %) and added to the PA hardener under vigorous stirring. The PA/Ch-TH2 was mixed with DGEB epoxy resin according to the recommend Wt. % (1:4 Wt. %) under continuous stirring. The solution was sprayed on a clean and rough (50 μm) steel panel to obtain dry film thickness 100 μm of epoxy composites coatings. The epoxy coatings on the steel panels were subjected to test their mechanical and anticorrosion performances after 7 days of curing at room temperature.

2.5. Evaluation Mechanical and Corrosion Resistance of Epoxy Ch-TH2 Composites Coating

Salt spray resistance of the epoxy-coated panels was conducted by using salt spray cabinet (CW Specialist equipment's Ltd. Model SF/450, Leominster, UK) at 35 °C under humidity 98% in the presence of seawater fog according to the American Society for Testing and Materials (ASTM B117-03) [20]. The corrosion resistance was evaluated according to the degree of rusting in relation to ASTM D610-95 [21]. The film hardness, impact resistance, the flexibility bend, abrasion resistance, and pull-off adhesion tests were carried out according ASTM D 3363-00 [22], ASTM D2794-04) [23], ASTM D 522-93a [24], ASTM D4060-19 [25], and ASTM D 4541-02 [26], respectively.

3. Results and Discussion

3.1. Preparation and Characterization of Ch-TH2

The present work aims to modify the chemical structure of chitosan to obtain mono-substituted chitosan from its reaction with cyanuric chloride (CC) at −10 °C in THF and K_2CO_3 to prevent chitosan crosslinking [27]. The mono-substituted chitosan cyanuric chloride (Ch-TC2) was reacted with hydrazine to obtain CH-TH2 as represented in Scheme 1. The reaction of chitosan with CC was obtained through the formation of strong covalent bonding between the amine group of chitosan and Cl group of CC. The same modification was reported on silica nanomaterials to apply as nano-filler for epoxy coatings to improve the mechanical properties of epoxy coatings [28]. The reaction yield of LCh-TC2 was greater than MCh-TC2 and HCh-TC2, which referred to increase solubility and lower viscosity of LCh. The good solubility of Ch-TC2 in hydrazine hydrate and CH_3CN indicate the formation of mono-substituted chitosan grafts rather than di or tri-substituted chitosan grafts that lead to crosslinked chitosan grafts.

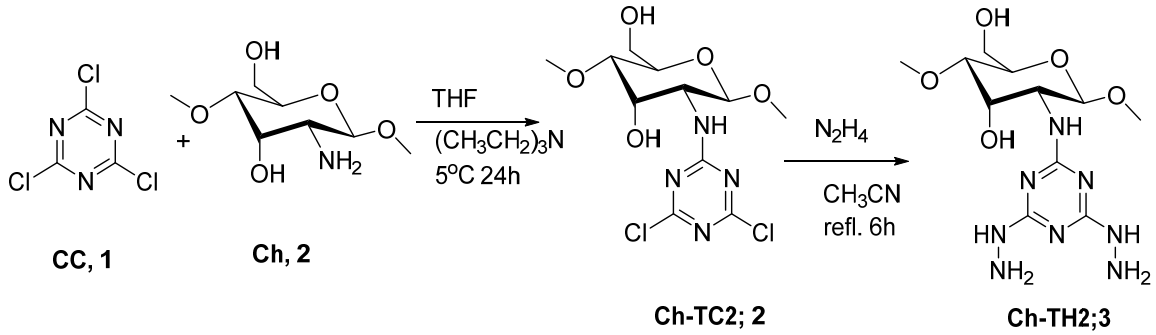

Scheme 1. Preparation of Ch-TH2.

The chemical structure of Ch-TH2 was identified from its ^{1}HNMR and FTIR spectra represented in Figures 1 and 2, respectively. The ^{1}HNMR spectra of HCh-TH2 and HCh were selected and listed in Figure 1a,b. The peaks of chitosan CH_2 and CH protons were clarified on its spectrum (Figure 1b) and agree with that reported before [29]. The new peaks at 4.23, 8.1, and 9.43 ppm of NH_2, NH attached to 1,3,5-triazine and NH of 4,6-dihydrazide, respectively, confirm the formation of Ch-TH2 (Figure 1b).

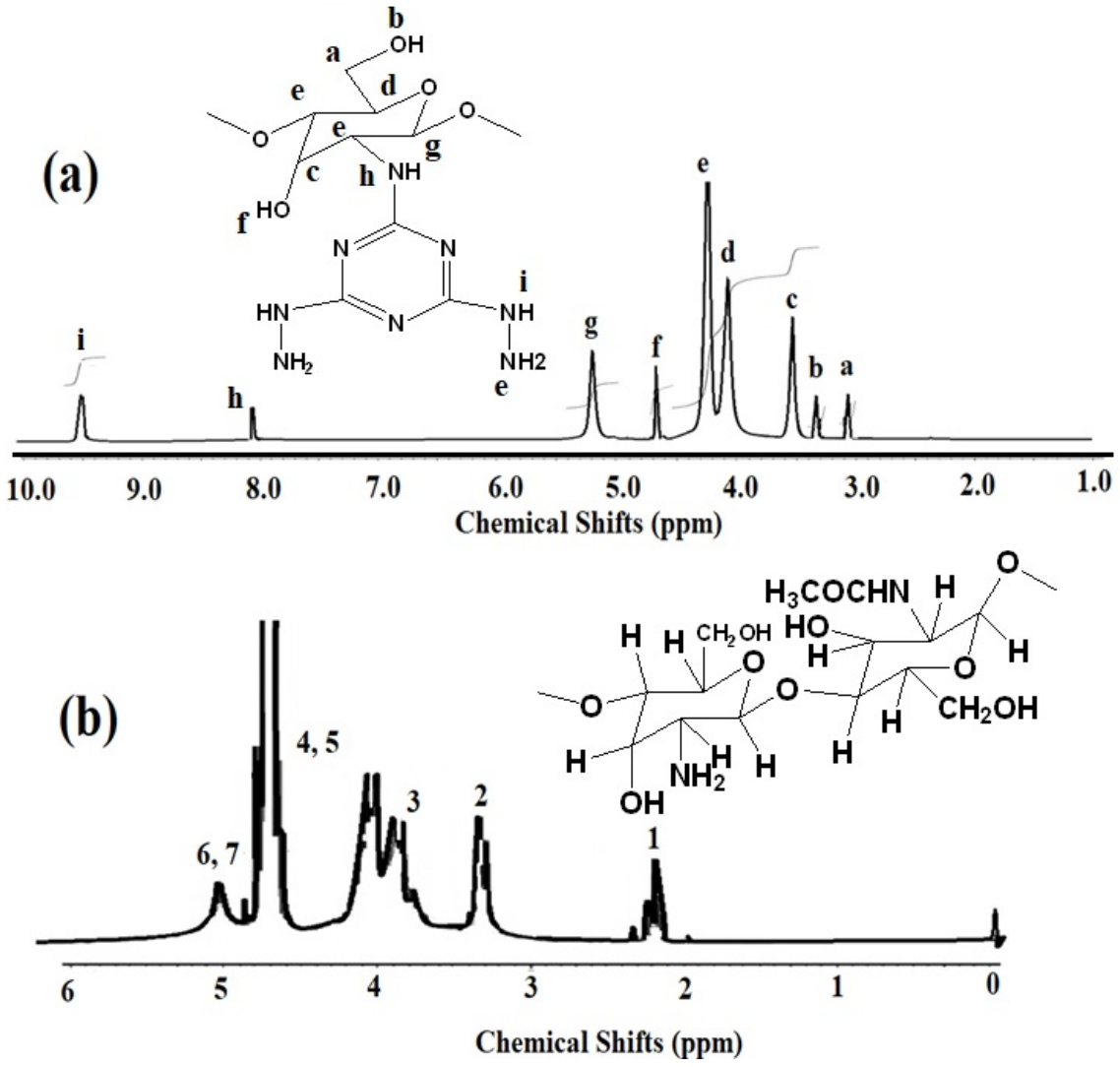

Figure 1. ^{1}HNMR spectrum of (**a**) chitosan modified with triazine dihydrazide moiety (HCh-TH2) and (**b**) high chitosan (HCh).

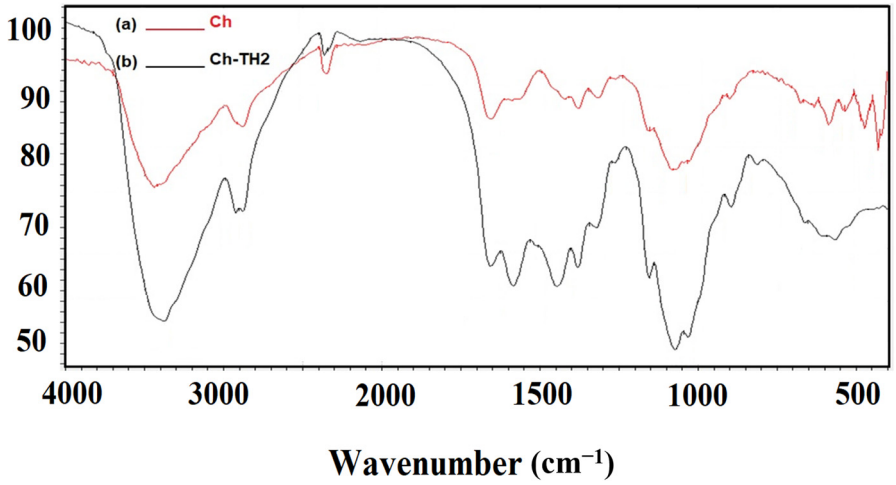

Figure 2. FTIR spectra of (**a**) chitosan and (**b**) HCh-TH2.

FTIR spectra of Ch and Ch-TH2 (Figure 2a,b) confirm the appearance of new strong absorption bands (Figure 2b) at 1665, 1560, and 1475 cm^{-1} that attributed to C=N stretching vibration, NH amides I and II, respectively [30]. These bands elucidate that the chitosan primary amines form covalent chemical bonding with cyanuric chloride, and the hydrazine was converted to hydrazide (Scheme 1). The presence of hydroxyl and NH groups in the chemical structures of CH and Ch-TH2 was confirmed from the appearance of broad bands from 3600 to 3200 cm^{-1} that referred to NH and OH stretching vibration (Figure 2a,b). The strong peak at 570 cm^{-1} (C–Cl stretching vibration), which appeared in the Ch-TC2 spectrum was disappeared from the Ch-TH2 spectrum (Figure 2b) to prove that the Cl groups were reacted with the amine group of chitosan and hydrazine. The band appeared at 1074 cm^{-1} assigned to C–O stretching, before and after modification was remained unchanged in both Ch and Ch-TH2 spectra (Figure 2a,b).

The thermal stability of modified chitosan with triazine hydrazide and % of triazine hydrazide grafts can be investigated from the Ch-TH2 thermogravimetric and differential thermogravimetric analysis (TGA-DTG) thermograms as represented in Figure 3a–d. The chitosan, LCh-TH2 and MCh-TH2 thermograms (Figure 3a,b,d, respectively) show a first degradation step (25–100 °C), which attributed to water loosely bound to chitosan polymers [31]. HCh-TH2 thermogram (Figure 3d) did not show this elimination step to elucidate its lower ability to bound water. The second main degradation step started from 280, 268, 260, and 240 °C for HCh-TH2, MCh-TH2, HCh, and LCh-TH2, respectively were represented their initial degradation temperature. These results confirm that the grafting of chitosan with triazine dihydrazide increased their thermal stability as well as increasing of chitosan molecular masses [32]. The degradation Wt. % of HCh-TH2, MCh-TH2, LCh-TH2, and Ch at 550 °C were 55, 60, 65, and 78%, respectively. Moreover, the remained residual Wt. % at 650 °C (RS%) was increased with the modification of chitosan with triazine dihydrazide and increasing the chitosan molecular masses. The RS% was referred to as the formation of crosslinked carbon and nitrogen cyclic structures. The RS% can be used to determine the percentage of grafting of chitosan with triazine dihydrazide as 23, 18, and 13% for HCh-TH2, MCh-TH2, and LCh-TH2, respectively. These values confirm that the increasing of chitosan molecular mass increased the amine group contents to increase its grafting % with CC (Scheme 1).

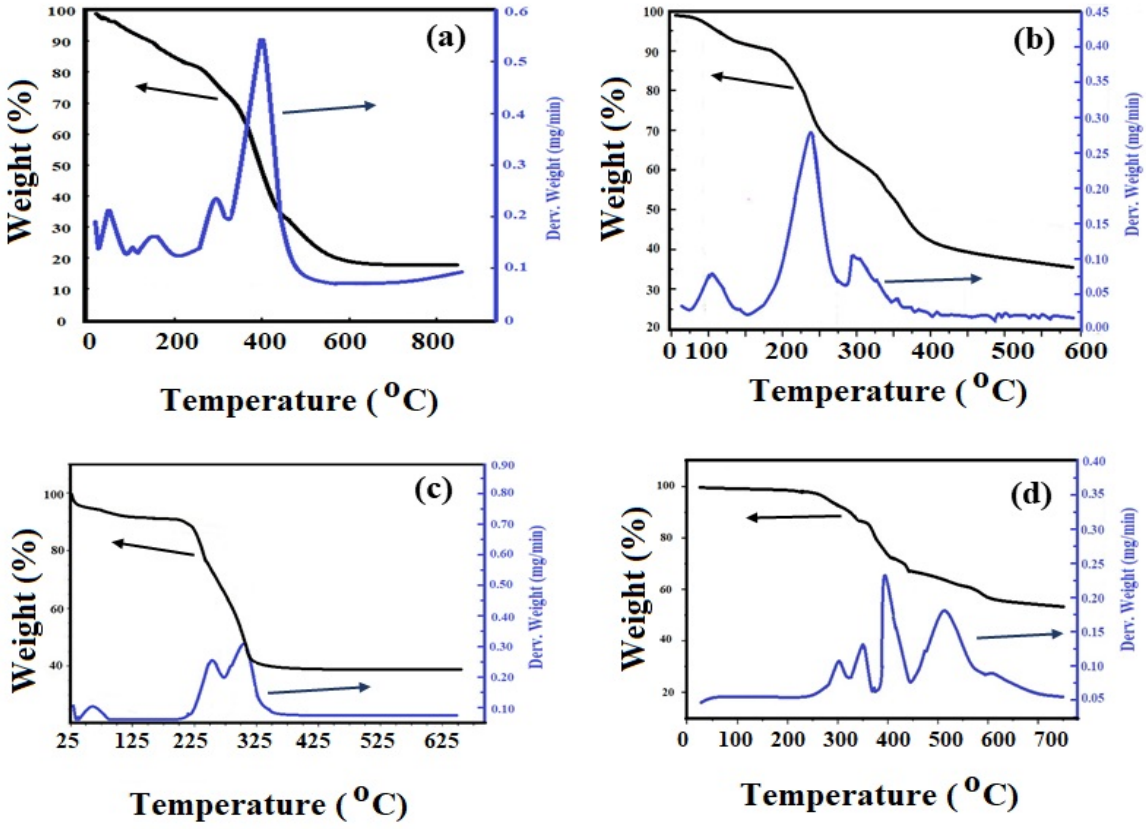

Figure 3. Thermogravimetric and differential thermogravimetric (TGA-DTG) thermograms of (**a**) HCh, (**b**) low chitosan (LCH)-TH2, (**c**) medium chitosan (MCh)-TH2, and (**d**) HCh-TH2 grafts.

The surface morphologies of Ch, HCh-TH2, and MCh-TH-2 were identified from their SEM micrographs summarized in Figure 4a–c. It is noticed that the grafting of Ch changed its surface morphologies from smooth (Figure 4a) to rough spherical surfaces (Figure 4b,c). The roughness of the Ch-TH2 was improved with the enhancement of chitosan molecular mass and changed the rough surfaces from pseudo-spherical to spherical structure (Figure 4b,c). This observation shows increased grafting percentages of chitosan with triazine hydrazide moiety [33].

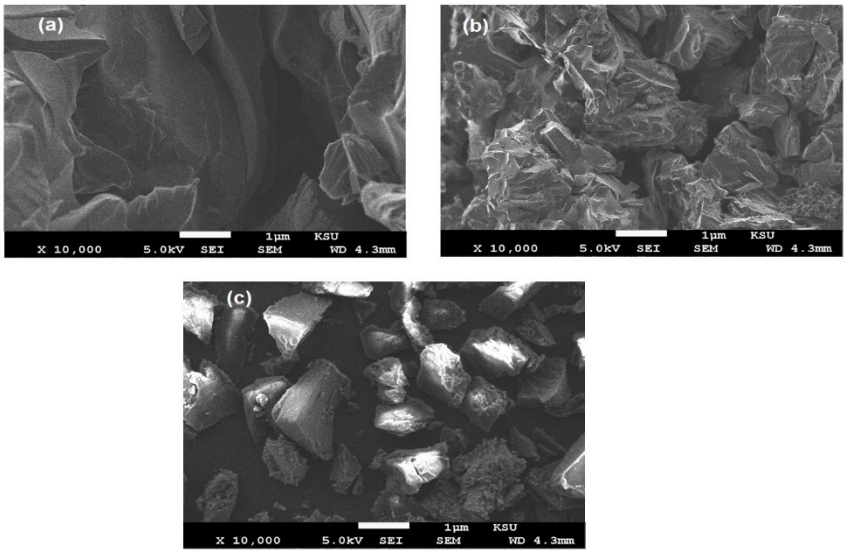

Figure 4. SEM micrographs of (**a**) HCh, (**b**) HCh-TH2, and (**c**) MCh-TH2.

The glass transition temperature values (T_g) of chitosan and its grafts with triazine dihydrazide Ch-TH2 can be determined from their differential scanning calorimeter (DSC) thermograms as represented in Figure 5. It was previously reported that the T_g of chitosan was affected by its molecular mass, crystallinity, deacetylation degree, water contents, sources, and/or method of extraction [34–37]. In this work, only HCh recorded a T_g value at 203 °C, which agrees with previously reported data [35]. In this respect, two cycles of heating and cooling runs were used to eliminate the degradation of absorbing moisture in the first run. The DSC thermograms' second run of LCh and MCh showed no significant stepwise increase in specific heat, and there was no evidence in favor of the occurrence of T_g value. The T_g values of LCh-TH2, MCh-TH2, and HCh-TH2 were 210, 193, and 182 °C, respectively (Figure 5). These values confirm that the grafting of triazine dihydrazide onto chitosan surfaces increased the flexibility of the chitosan polymer chains rather than water humidity that was eliminated in the first heating run. The higher triazine dihydrazide contents into HCh-TH2 and MCh-TH2 reduced T_g values due to mismatching triazine hydrazide groups (C=N and NH) with hydrogen bonding [38]. The lower contents of triazine dihydrazide in LCh-TH2 increased the chitosan stiffness and restricted the molecular mobility due to the asymmetrically structure of LCh besides low triazine hydrazide contents [39].

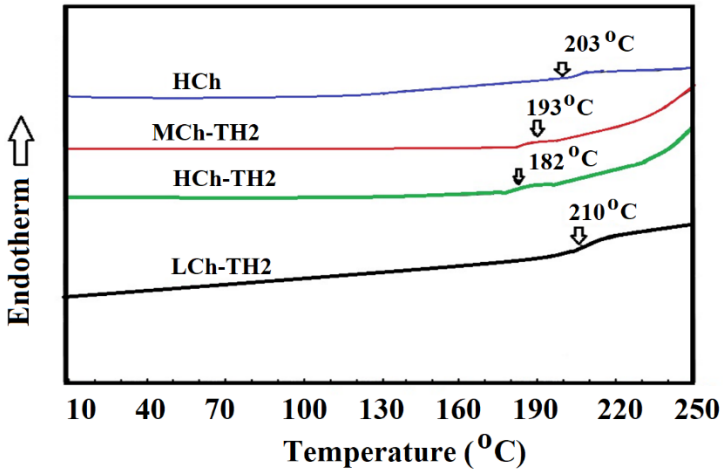

Figure 5. DSC thermograms of Ch-TH2 derivatives.

3.2. Curing of Epoxy in the Presence of Ch-TH2 Derivatives

The curing of epoxy resin based on DGEB with a polyamine (PA) produces highly tough crosslinked networks due to high PA crosslinking reactivity with epoxy resin [40]. The higher crosslinking densities of cured epoxy resins produced films having micro-, nano-cracks, and holes. The present work aims to modify the chemical structures of chitosan with new functional primary, secondary, and tertiary amine groups to improve the mechanical properties of epoxy resin. It was previously reported that the chitosan, which was blended during the curing of the epoxy with PA hardener, improved its coatings performances [41]. In the present work, the chemical structure of chitosan amine groups was modified with triazine hydrazide groups (Scheme 1) to activate the curing reaction for DGEB epoxy ring-opening with PA. The HCh-TH2, MCh-TH2, or LCh-TH2 were added with suitable weight ratios ranged from 1 to 10 Wt. % during the curing of DGEB/PA, as reported in the experimental section. The SEM images of the fractured cured films based on DGEB/PA (blank) in the presence of 3, 6, and 10 Wt. % of HCh-TH2 were selected and presented in Figure 6a–d. It was noticed that the microcracks and holes were observed during the curing of the DGEB/PA blank (Figure 6a). The cured DGEB/PA in the presence of 3–6 Wt. % of HCh-TH2 consisted of a homogeneous and uniform structure (Figure 6b,c). The increasing of HCh-TH2 up to 10 Wt. % (Figure 6d) produces heterogeneous epoxy networks with the appearance of some cracks. These data confirm that the curing of DGEB/PA was affected by the concentration of Ch-TH2 at different weight ratios as well as surface morphology.

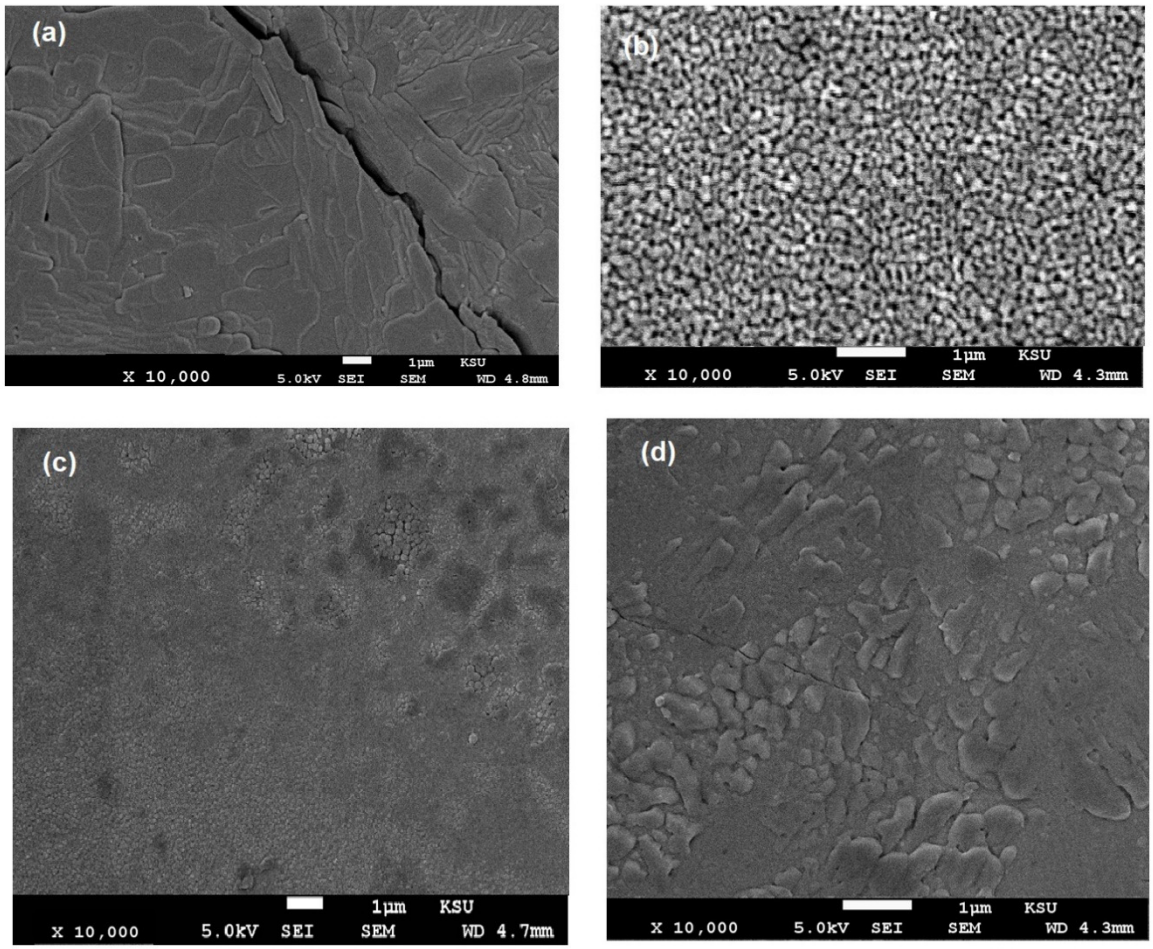

Figure 6. SEM micrographs of DGEB/PA films modified with different Wt. % of HCh-TH2 (**a**) 0, (**b**) 3, (**c**) 6, and (**d**) 10 Wt. %.

The curing exothermic of DGEB/PA in the absence and presence of HCh-TH2, MCh-TH2, or LCh-TH2 was investigated from non-isothermal dynamic DSC measurements at a heating rate 5 °C min^{-1} as represented in Figure 7a–c. These conditions were selected as moderate conditions [35,36] to investigate the effect of molecular masses and grafting contents of chitosan with triazine dihydrazide on curing of DGEB/PA system. The thermograms show unimodal-like patterns to confirm that the curing exothermic reactions were carried out with single-step kinetics. The total exothermic heat evolved (ΔH) from the curing reactions of DGEB/PA as blank and in the presence of different Wt. % of HCh-TH2, MCh-TH2, or LCh-TH2 were calculated from the area under peaks (Figure 7a–c) and represented in Table 1. Careful inspection of the DGEB/PA curing data (Table 1 and Figure 7a–c) proves that the addition of HCh-TH2, MCh-TH2, or LCh-TH2 decreased their onset curing temperatures except at 10 Wt. %. Moreover, the curing reaction enthalpy of the DGEB/PA system were increased with increasing Ch contents (Table 1). These data mean that the grafting of chitosan with new primary, secondary, and tertiary N atoms accelerates the curing process of DGEB/PA. The triazine groups facilitates the N atoms to use their lone pair of electrons to act as a curing catalyst or co-curing agent with PA hardener. The catalytic behavior Ch-TH2 was confirmed from the appearance of shoulder peaks in the curing curves of DGEB/PA at a lower temperature in the presence of 3 Wt. % of Ch-TH2 (Figure 7a–c) [42,43]. The glass transition temperatures after dynamic curing (T_g) were recorded from DSC thermograms (Figure 7a–c) and are summarized for all systems in Table 1. It was obviously seen that the blank DGEB/PA epoxy thermoset had the highest T_g value of 110 °C than that cured in the presence of Ch-TH2 up to 6 Wt. %. The increasing of Ch-TH2 content up to 10 Wt. % during the curing

of DGEB/PA increases its T_g value that referred to increasing the crosslinking densities and rigidity of the cured DGEB/PA. This means that the cured DGEB/PA epoxy film was believed to possess flexible networks with the incorporation of Ch-TH2 up to 6 Wt. %, as confirmed from the lowering of their T_g values. Increasing Ch-TH2 contents up to 10 Wt. % increased the T_g and ΔH values of the DGEB/PA system to confirm the increasing of the crosslinking density of the epoxy.

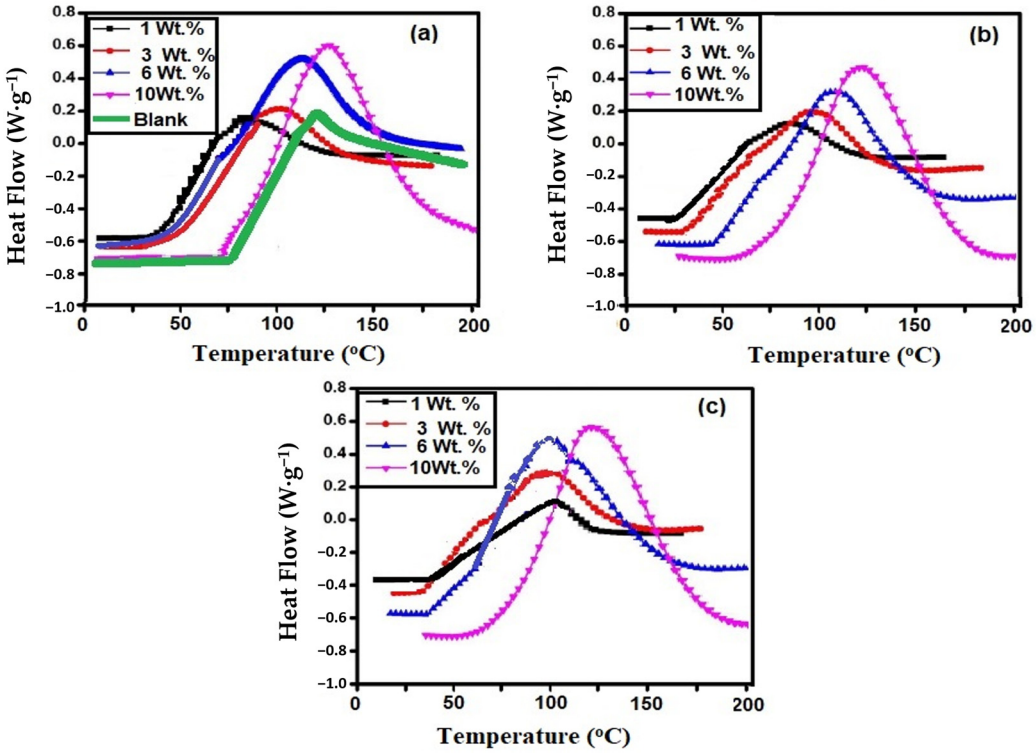

Figure 7. Non-isothermal DSC thermograms of the cured DGEB/PA in the presence of different Wt. % of (**a**) LCh-TH2, (**b**) MCh-TH2 and (**c**) HCh-TH2.

Table 1. DSC data of DGEB/polyamine (PA) at a heating rate of 5 °C·min^{-1} in the absence and presence of different Wt. % of Ch-TH2.

DGEB/PA Modified with Ch-TH2 Wt. %		T_g After Curing (°C)	ΔH J·g^{-1}	Onset Temperature (°C)	Maximum Temperature (°C)
Blank		110	260	115	190
HCh-TH2	1	100	350	120	219
	3	95	355	100	215
	6	89	365	98	207
	10	115	390	125	200
MCh-TH2	1	95	320	85	190
	3	90	325	95	180
	6	98	355	110	195
	10	110	370	120	200
LCh-TH2	1	90	300	85	180
	3	95	310	100	190
	6	105	315	110	190
	10	128	320	135	195

The curing data summarized in Table 1 prove the proposed curing reaction mechanism of the DGEB/PA system in the presence of Ch-TH2, as shown in Scheme 2. The presence of primary amine in non-modified chitosan and modified chitosan with triazine hydrazide Ch-TH2 activated their linking into epoxy networks (Scheme 2). The chemical linking of Ch-TH2 into epoxy networks improved the incorporation of the spacer group inside the DGEB/PA matrix. Moreover, the presence of tertiary amine group inside the triazine ring facilitated the curing reaction as indicated from the increasing of Δ H value with increasing chitosan molecular masses and triazine hydrazide contents.

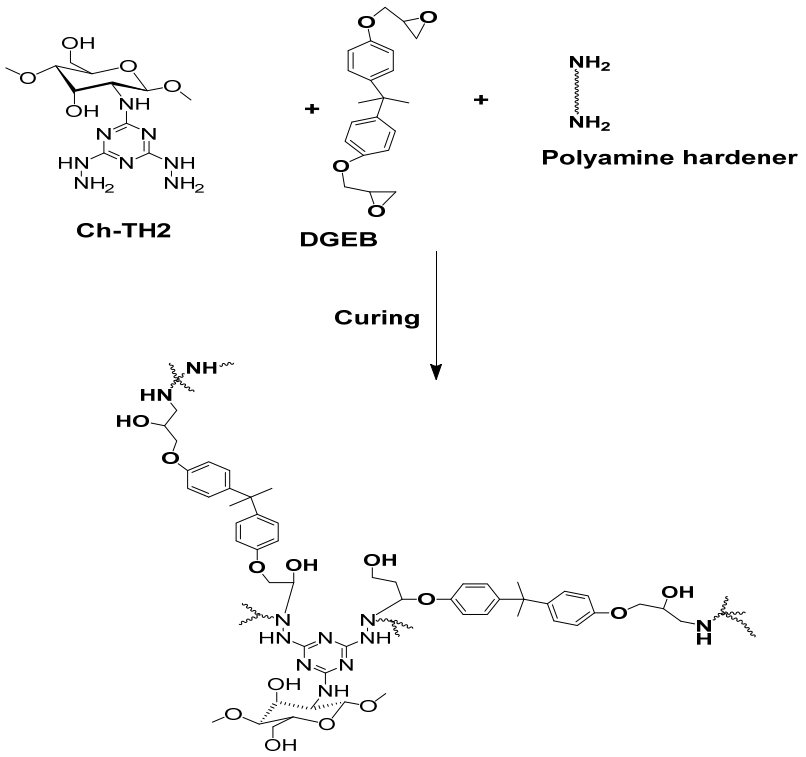

Scheme 2. Curing of DGEB/PA in the presence of Ch-TH2.

3.3. Mechanical and Durability of DGEB/PA in the Presence of Ch-TH2 as Organic Coatings

The commercial cured epoxy coating is preferred for steel protection in the marine environment due to its good adhesion on the steel surfaces besides its barrier effect as an anticorrosive layer. An improvement in its adhesion and mechanical properties and barrier effect could be helpful in improving its capability in corrosion protection. In this respect, the curing mechanism (Scheme 2) of the DGEB/PA confirms that there is an additional hydroxyl group produced from the reaction of amine groups of LCh-TH2, MCh-TH2, or HCh-TH2 with epoxy resin. It is well established that the increasing of hydroxyl group contents in the cured epoxy films improves their adhesion with steel surface [44]. In this respect, the pull-off adhesion strengths of epoxy coating on the steel surfaces with the incorporation of LCh-TH2, MCh-TH2, or HCh-TH2 were measured and are summarized in Table 2. The results were compared with the reported data for using non-modified chitosan with epoxy coatings [34]. The adhesion data elucidate that the modification of chitosan into LCh-TH2, MCh-TH2, or HCh-TH2 increased the epoxy films adhesion strengths more than blank and that blended with chitosan only (Table 1). These observations confirm that the presence of hydrazide and triazine groups in the chemical structures of LCh-TH2, MCh-TH2, or HCh-TH2 besides the hydroxyl groups produced from curing (Scheme 2) improves their chelation with metallic surfaces [45]. The increasing of triazine hydrazide contents in the order HCh-TH2 > MCh-TH2 > LCh-TH2 (TGA-DTG curves; Figure 3b–d) improves the adhesion of modified epoxy films in the same order.

Table 2. Mechanical properties of cured DGEB/PA epoxy films in the absence and presence of different Wt. % of LCh-TH2, MCh-TH2, or HCh-TH2 loading.

Coating Design	Nanoparticles Weight % (Wt. %)	Hardness (Newton)	Adhesion (MPa)	Impact (Joule)	Pending	Abrasion Resistance Weight Loss (mg)/2000 Cycles
Blank epoxy	0	5 ± 0.1	5 ± 1.8	5 ± 0.2	Pass	110 ± 2.2
HCh-TH2	1	8 ± 0.3	8 ± 0.2	8 ± 0.1	Pass	45 ± 1.4
	3	10 ± 0.2	12 ± 1.1	10 ± 0.3	Pass	28 ± 1.1
	6	12 ± 0.1	14 ± 1.4	13 ± 0.1	Pass	15 ± 2.1
	10	14 ± 0.2	17 ± 0.6	12 ± 0.2	Pass	20 ± 1.8
MCh-TH2	1	6 ± 0.1	7 ± 1.4	7 ± 0.3	Pass	55 ± 1.1
	3	8 ± 0.1	10 ± 0.2	9 ± 0.2	Pass	30 ± 1.4
	6	11 ± 0.1	12 ± 0.2	11 ± 0.2	Pass	20 ± 0.2
	10	10 ± 0.3	14 ± 0.2	10 ± 0.3	Pass	25 ± 1.4
LCh-TH2	1	5 ± 0.2	6 ± 0.2	6 ± 0.3	Pass	65 ± 1.1
	3	6 ± 0.2	7 ± 0.2	8 ± 0.2	Pass	38 ± 0.2
	6	9 ± 0.3	9 ± 1.4	10 ± 0.2	Pass	23 ± 1.4
	10	12 ± 0.1	13	10 ± 0.3	Pass	32 ± 1.1
MCh/epoxy [35]	3	5 ± 0.2	6 ± 1.4	7 ± 0.3	Pass	40 ± 1.1
	6	8 ± 0.1	8 ± 1.4	9 ± 0.3	Pass	25 ± 2.1
	10	11 ± 0.2	11 ± 1.4	12 ± 0.3	Pass	30 ± 1.8

The increasing of epoxy adhesion strengths on the steel surfaces improved their mechanical properties, such as measured impact strength, scratch hardness strength, bending, and abrasion resistance, as summarized in Table 2.

The improvement in bending, impact, and abrasion resistance with increasing Ch-TH2 molecular masses and contents confirmed that the modification of chitosan with triazine hydrazide offers a flexible, biocompatible platform for designing coatings to protect surfaces from mechanical damages [46]. Moreover, the increasing of Ch-TH2 molecular masses and content also improved the scratch hardness of cured epoxy films reflected on the cohesive strength of the coated film. The SEM micrograph of DGEB/PA blank (Figure 6a) elucidated the presence of holes among the coating layer that responsible for poor mechanics of the cured film. The incorporation of Ch-TH2 during the curing of DGEB/PA using 3 Wt. % (Figure 6b) and 6 Wt. % (Figure 6c) produced more uniform epoxy layers with the disappearance of micro or nano-holes. The uniform epoxy films with increasing of HCh-TH2 to 3 and 6 Wt. % (Figure 6b,c) was responsible for the improvement in impact, abrasion resistances of all epoxy films treated with LCh-TH2, MCh-TH2, or HCh-TH2. The appearance of thin holes between the epoxy layer with the incorporation of HCh-TH2 10 Wt. % (Figure 6d) reduced its abrasion resistance. This result also confirmed the decreasing impact and increasing weight loss from epoxy films with HCh-TH2 10 Wt. % (Table 2).

The salt spray is recommended as an accelerated corrosion evaluation test compared with electrochemical impedance spectroscopy (EIS), but salt spray is often specified but rarely corresponds well to service degradation [47]. The ISO 12944 and the NORSOK M-501 standards propose a salt spray test among several accelerated aging tests to evaluate the coatings' anticorrosive property and durability [48]. The salt spray resistances of DGEB/PA in the absence and presence of LCh-TH2, MCh-TH2, or HCh-TH2 coated on the steel surface were evaluated as an anticorrosion accelerated test for epoxy coatings having mechanical damage (X-cut). The amount of the formed rusting beneath or through a coated epoxy film is used to evaluate whether a coating system should be repaired or

replaced [21]. In this respect, the area of the rust formed under the coating system was evaluated as a percentage when compared with the total area of the coated panel to determine the amount and distribution of visible surface rust. The percentage of the rusting area related to the total coated area was evaluated using a zero to ten scale, based on the percentage of visible surface rust [21]. Moreover, the distribution of the rust was also classified as spot rust, general rust, pinpoint rust, or hybrid rust. The failure of the salt spray test was recorded for adhesion loss coatings due to blistering or rusting after exposure time to seawater fog. The rusts under coatings occurred from the water, oxygen, and salt diffusions from the coatings to steel surfaces to lose the adhesion forces between the coating layer and steel surfaces. In this respect, the epoxy coated on the steel panels photos and salt spray resistance data were determined and are represented in Figure 8a–d and Table 3. The data of epoxy coatings in the presence of chitosan are listed in Table 3 as comparative data [34]. The data show that DGEB/PA, in the absence of chitosan or their modifications, achieved salt spray resistivity up to 500 h (Figure 8a, Table 3). This means that the presence of micro-cracks or holes in the epoxy surfaces increased the diffusion of corrosive water, salts, and oxygen to form rust under coatings. The presence of LCh-TH2, MCh-TH2, or HCh-TH2 (1 Wt. %) increased the salt spray exposure times of the epoxy coatings up to 750 h (Table 3, Figure 8b–d). This means that there was an improvement in the epoxy surfaces' morphologies (Figure 6) with the incorporation of LCh-TH2, MCh-TH2, or HCh-TH2 in the epoxy networks (Scheme 2). The increasing of Wt. % of LCh-TH2, MCh-TH2, or HCh-TH2 in the DGEB/PA improved the corrosion resistivity and salt spray exposure time to 1500 h (Figure 8b–d, Table 3). Moreover, the addition of 6 Wt. % of LCh-TH2, MCh-TH2, or HCh-TH2 during the curing of DGEB/PA increased their anticorrosion and salt spray resistance in a marine aggressive seawater environment up to 2000 h (Table 3; Figure 8b–d). It was noticed that the increasing molecular masses of chitosan and triazine hydrazide percentages increased their incorporation in the epoxy matrix with forming homogeneous networks with the absence of holes or micro-cracks in the DGEB/PA coatings (Figure 6). The increase in LCh-TH2, MCh-TH2, or HCh-TH2 to 10 Wt. % during the curing of epoxy affected and reduced the anticorrosion performances of epoxy coating to salt spray to 1000 h (Figure 8b–d; Table 3). Moreover, the salt spray resistivity of the epoxy coatings was ordered as LCh-TH2 > MCh-TH2 > HCh-TH2, which attributed to the formation of some nano-cracks in the epoxy with the formation of heterogeneous epoxy networks in the case of HCh-TH2 (10 Wt. %). Accordingly, the formation of homogeneous and flexible epoxy networks in the presence of Ch-TH2 tended to reduce the diffusion of aggressive corrosive species from the epoxy to steel surfaces even with the presence of mechanical damages (X-cut). This was referred to as the presence of triazine and hydrazide groups, as a graft on chitosan surfaces linked with the epoxy network was responsible for their chelation with steel surfaces. There were some non-covalent interactions, such as hydrogen bonding and electrostatic interactions between Ch-TH2 (positively charged when added in acetic acid during the curing process) and negative charges of epoxy OH groups. Owing to the reversible nature of the non-covalent networks and the cooperation of these interactions, these networks exhibit rapid network recovery, high stretchability, and efficient autonomy to fill the damaged area as anticorrosive layers [49].

Table 3. Salt spray resistance of DGEB/PA epoxy coating films at different Ch-TH2 loading after exposure to salt spray fog at different times.

Coating Design	Exposure Time (h)	Nanoparticles Weight % (Wt. %)	Disbanded Rust Area %	Rating Number of Coating Area (ASTM D610) [22]
Blank epoxy	550	0	19 ± 0.1	5
HCh-TH2	750	1	5 ± 0.05	7
	1500	3	6 ± 0.08	7
	2000	6	1 ± 0.08	9
	1000	10	8 ± 0.04	7

Table 3. *Cont.*

Coating Design	Exposure Time (h)	Nanoparticles Weight % (Wt. %)	Disbanded Rust Area %	Rating Number of Coating Area (ASTM D610) [22]
MCh-TH2	750	1	12 ± 0.04	6
	1500	3	10 ± 0.04	6
	2000	6	7 ± 0.08	7
	1000	10	6 ± 0.08	7
LCh-TH2	750	1	20 ± 0.1	5
	1500	3	15 ± 0.04	6
	2000	6	10 ± 0.04	6
	1000	10	2 ± 0.08	8
MCh/epoxy [35]	550	3	Not reported	4
	550	6	Not reported	5
	550	10	Not reported	6

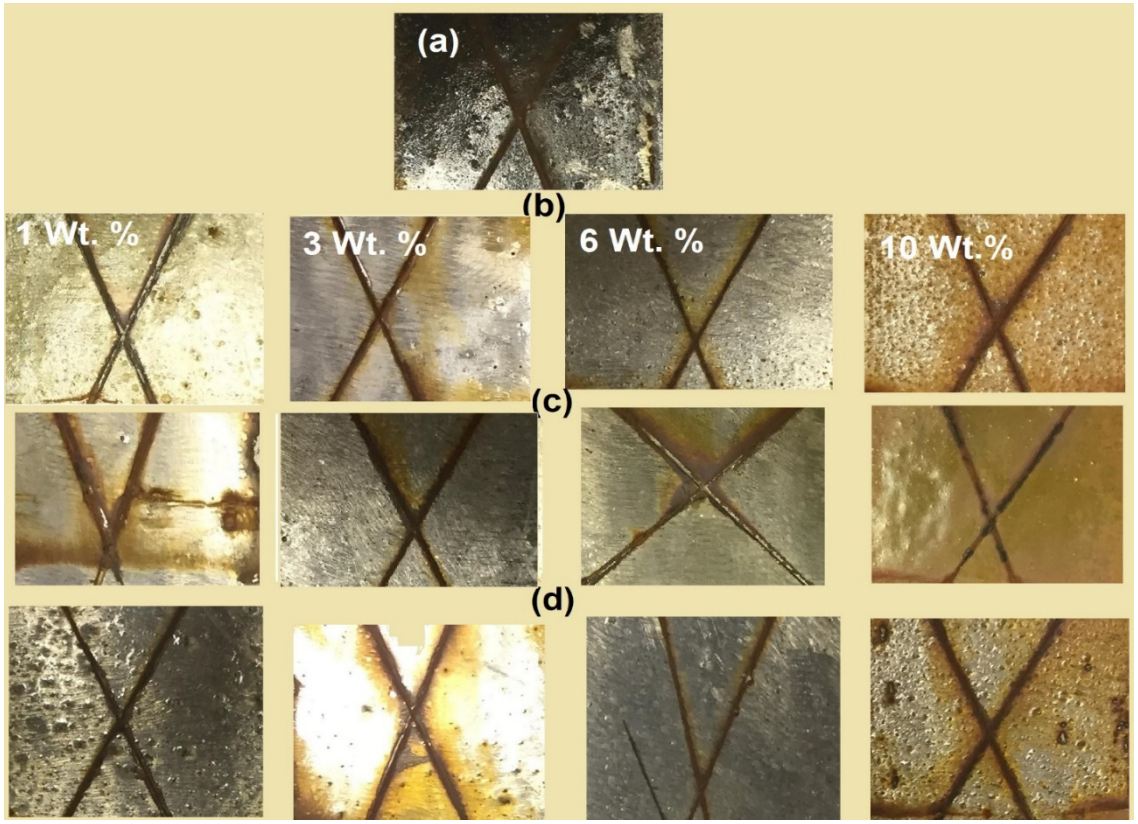

Figure 8. Salt spray resistance photos of epoxy coating mixed with different Wt. % of (**a**) 0, (**b**) HCh-TH2, (**c**) MCh-TH2, and (**d**) LCh-TH2 at different exposure times.

4. Conclusions

Different molecular masses of chitosan modified with triazine hydrazide to act as activator and linker for epoxy networks having superior mechanical and anticorrosive coatings for steel substrate. The thermal stability of chitosan was improved by increasing its molecular masses and modification percentages with triazine hydrazide grafts. Uniform cured epoxy surface morphology without the formation of microcracks or holes occurred with increasing Ch-TH2 up to 6 Wt. % to obtain superior

mechanical properties. Flexible chains based on chitosan triazine hydrazide grafts were cured with epoxy matrices to reduce the T_g of the blank epoxy from 110 to 89 °C, and they were responsible for high impact and abrasion resistance of epoxy coatings. Higher salt spray resistance was achieved after exposure of modified epoxy with HCh-TH2 (6 Wt. %) that attributed to the reversible nature of the non-covalent networks having rapid network recovery, high stretchability, and efficient autonomy to fill the damaged area as anticorrosive layers.

Author Contributions: Conceptualization, A.M.A. and A.E.-F.; methodology, A.O.E.; software, A.O.E.; validation, A.M.A.; formal analysis, A.M.A.; investigation, A.M.A.; resources, A.M.A. and H.A.A.-L.; data curation, A.M.A.; writing—original draft preparation, A.M.A.; writing—review and editing, A.M.A., A.E.-F. and H.A.A.-L.; visualization, A.M.A.; supervision, H.A.A.-L. and A.M.A.; project administration A.M.A.; funding acquisition, A.M.A. All authors have read and agreed to the published version of the manuscript.

Funding: This research was funded by Deanship of Scientific Research at King Saud University (RG-1441-235).

Acknowledgments: The authors extend their appreciation to the Deanship of Scientific Research at King Saud University for funding this work through research group No. (RG-1441-235).

Conflicts of Interest: The authors declare no conflict of interest.

References

1. Ashassi-Sorkhabi, H.; Kazempour, A. Chitosan, its derivatives and composites with superior potentials for the corrosion protection of steel alloys: A comprehensive review. *Carbohydr. Polym.* **2020**, *237*, 116110. [CrossRef] [PubMed]
2. John, S.; Joseph, A.; Jose, A.J.; Narayana, B. Enhancement of corrosion protection of mild steel by chitosan/ZnO nanoparticle composite membranes. *Prog. Org. Coat.* **2015**, *84*, 28–34. [CrossRef]
3. Zheludkevich, M.; Tedim, J.; Freire, C.; Fernandes, S.C.; Kallip, S.; Lisenkov, A.; Gandini, A.; Ferreira, M. Self-healing protective coatings with "green" chitosan based pre-layer reservoir of corrosion inhibitor. *J. Mater. Chem.* **2011**, *21*, 4805–4812. [CrossRef]
4. Atta, A.M.; El-Mahdy, G.A.; Al-Lohedan, H.A.; Ezzat, A.-R.O. Synthesis of nonionic amphiphilic chitosan nanoparticles for active corrosion protection of steel. *J. Mol. Liq.* **2015**, *211*, 315–323. [CrossRef]
5. Shibata, M.; Fujigasaki, J.; Enjoji, M.; Shibita, A.; Teramoto, N.; Ifuku, S. Amino acid-cured bio-based epoxy resins and their biocomposites with chitin-and chitosan-nanofibers. *Eur. Polym. J.* **2018**, *98*, 216–225. [CrossRef]
6. Kiuchi, H.; Kai, W.; Inoue, Y. Preparation and characterization of poly (ethylene glycol) crosslinked chitosan films. *J. Appl. Polym. Sci.* **2008**, *107*, 3823–3830. [CrossRef]
7. Illy, N.; Benyahya, S.; Durand, N.; Auvergne, R.; Caillol, S.; David, G.; Boutevin, B. The influence of formulation and processing parameters on the thermal properties of a chitosan–epoxy prepolymer system. *Polym. Int.* **2014**, *63*, 420–426. [CrossRef]
8. Shibata, M.; Enjoji, M.; Sakazume, K.; Ifuku, S. Bio-based epoxy/chitin nanofiber composites cured with amine-type hardeners containing chitosan. *Carbohydr. Polym.* **2016**, *144*, 89–97. [CrossRef]
9. Li, Y.; Xiao, F.; Moon, K.S.; Wong, C. Novel curing agent for lead-free electronics: Amino acid. *J. Polym. Sci. Part A Polym. Chem.* **2006**, *44*, 1020–1027. [CrossRef]
10. Wang, M.; Xue, H.; Feng, Z.; Cheng, B.; Yang, H. Increase of tensile strength and toughness of bio-based diglycidyl ether of bisphenol A with chitin nanowhiskers. *PLoS ONE* **2017**, *12*, e0177673. [CrossRef]
11. Selvam, V.; Kumar, M.S.C.; Vadivel, M. Mechanical properties of epoxy/chitosan biocomposites. *Int. J. Chem. Sci.* **2013**, *11*, 1103–1109.
12. Atay, H.Y.; Doğan, L.E.; Çelik, E. Investigations of self-Healing property of chitosan-reinforced epoxy dye composite coatings. *J. Mater.* **2013**, *2013*, 613717.
13. Ma, I.W.; Sh, A.; Ramesh, K.; Vengadaesvaran, B.; Ramesh, S.; Arof, A.K. Anticorrosion properties of epoxy-nanochitosan nanocomposite coating. *Prog. Org. Coat.* **2017**, *113*, 74–81.
14. Ruhi, G.; Modi, O.; Dhawan, S. Chitosan-polypyrrole-SiO_2 composite coatings with advanced anticorrosive properties. *Synth. Met.* **2015**, *200*, 24–39. [CrossRef]

15. Ashassi-Sorkhabi, H.; Bagheri, R.; Rezaei-moghadam, B. Sonoelectrochemical synthesis of ppy-MWCNTs-chitosan nanocomposite coatings: Characterization and corrosion behavior. *J. Mater. Eng. Perform.* **2015**, *24*, 385–392. [CrossRef]
16. Chauhan, D.S.; Quraishi, M.; Sorour, A.; Saha, S.K.; Banerjee, P. Triazole-modified chitosan: A biomacromolecule as a new environmentally benign corrosion inhibitor for carbon steel in a hydrochloric acid solution. *RSC Adv.* **2019**, *9*, 14990–15003. [CrossRef]
17. Ansari, K.; Chauhan, D.S.; Quraishi, M.; Mazumder, M.A.; Singh, A. Chitosan Schiff base: An environmentally benign biological macromolecule as a new corrosion inhibitor for oil & gas industries. *Int. J. Biol. Macromol.* **2020**, *144*, 305–315.
18. Sambyal, P.; Ruhi, G.; Dhawan, S.; Bisht, B.; Gairola, S. Enhanced anticorrosive properties of tailored poly (aniline-anisidine)/chitosan/SiO_2 composite for protection of mild steel in aggressive marine conditions. *Prog. Org. Coat.* **2018**, *119*, 203–213. [CrossRef]
19. Pozzo, L.d.Y.; da Conceição, T.F.; Spinelli, A.; Scharnagl, N.; Pires, A.T.N. The influence of the crosslinking degree on the corrosion protection properties of chitosan coatings in simulated body fluid. *Prog. Org. Coat.* **2019**, *137*, 105328. [CrossRef]
20. ASTM International. *ASTM B117-19, Standard Practice for Operating Salt Spray (Fog) Apparatus*; ASTM International: West Conshohocken, PA, USA, 2019.
21. ASTM International. *ASTM D610-08(2019), Standard Practice for Evaluating Degree of Rusting on Painted Steel Surfaces*; ASTM International: West Conshohocken, PA, USA, 2019.
22. ASTM International. *ASTM D3363-00, Standard Test Method for Film Hardness by Pencil Test*; ASTM International: West Conshohocken, PA, USA, 2000.
23. ASTM International. *ASTM D2794-93(2004), Standard Test Method for Resistance of Organic Coatings to the Effects of Rapid Deformation (Impact)*; ASTM International: West Conshohocken, PA, USA, 2004.
24. ASTM International. *ASTM D522-93a, Standard Test Methods for Mandrel Bend Test of Attached Organic Coatings*; ASTM International: West Conshohocken, PA, USA, 2001.
25. ASTM International. *ASTM D4060-19, Standard Test Method for Abrasion Resistance of Organic Coatings by the Taber Abraser*; ASTM International: West Conshohocken, PA, USA, 2019.
26. ASTM International. *ASTM D4541-02, Standard Test Method for Pull-Off Strength of Coatings Using Portable Adhesion Testers*; ASTM International: West Conshohocken, PA, USA, 2002.
27. Zargarkazemi, A.; Sadeghi-Kiakhani, M.; Arami, M.; Bahrami, S.H. Modification of wool fabric using prepared chitosan-cyanuric chloride hybrid. *J. Text. Inst.* **2015**, *106*, 80–89. [CrossRef]
28. Maqbool, M.; Manral, A.; Jameel, E.; Kumar, J.; Saini, V.; Shandilya, A.; Tiwari, M.; Hoda, N.; Jayaram, B. Development of cyanopyridine–triazine hybrids as lead multitarget anti-Alzheimer agents. *Bioorgan. Med. Chem.* **2016**, *24*, 2777–2788. [CrossRef] [PubMed]
29. Lavertu, M.; Xia, Z.; Serreqi, A.; Berrada, M.; Rodrigues, A.; Wang, D.; Buschmann, M.; Gupta, A. A validated 1H NMR method for the determination of the degree of deacetylation of chitosan. *J. Pharm. Biomed. Anal.* **2003**, *32*, 1149–1158. [CrossRef]
30. Ranjbar-Mohammadi, M.; Arami, M.; Bahrami, H.; Mazaheri, F.; Mahmoodi, N.M. Grafting of chitosan as a biopolymer onto wool fabric using anhydride bridge and its antibacterial property. *Colloids Surf. B Biointerfaces* **2010**, *76*, 397–403. [CrossRef]
31. Wanjun, T.; Cunxin, W.; Donghua, C. Kinetic studies on the pyrolysis of chitin and chitosan. *Polym. Degrad. Stab.* **2005**, *87*, 389–394. [CrossRef]
32. Mucha, M.; Pawlak, A. Complex study on chitosan degradability. *Polim. Wars.* **2002**, *47*, 509–516. [CrossRef]
33. Gómez-Mascaraque, L.G.; Sanchez, G.; López-Rubio, A. Impact of molecular weight on the formation of electrosprayed chitosan microcapsules as delivery vehicles for bioactive compounds. *Carbohydr. Polym.* **2016**, *150*, 121–130. [CrossRef]
34. Neto, C.d.T.; Giacometti, J.A.; Job, A.E.; Ferreira, F.C.; Fonseca, J.L.C.; Pereira, M.R. Thermal analysis of chitosan based networks. *Carbohydr. Polym.* **2005**, *62*, 97–103. [CrossRef]
35. Sakurai, K.; Maegawa, T.; Takahashi, T. Glass transition temperature of chitosan and miscibility of chitosan/poly (N-vinyl pyrrolidone) blends. *Polymer* **2000**, *41*, 7051–7056. [CrossRef]
36. Ma, X.; Qiao, C.; Wang, X.; Yao, J.; Xu, J. Structural characterization and properties of polyols plasticized chitosan films. *Int. J. Biol. Macromol.* **2019**, *135*, 240–245. [CrossRef]

37. Dong, Y.; Ruan, Y.; Wang, H.; Zhao, Y.; Bi, D. Studies on glass transition temperature of chitosan with four techniques. *J. Appl. Polym. Sci.* **2004**, *93*, 1553–1558. [CrossRef]
38. Marcos, A.; Rodriguez, A.; González, L. Dynamic properties of copolyetherureas. *J. Non-Cryst. Solids* **1994**, *172*, 1125–1129. [CrossRef]
39. Barszczewska-Rybarek, I.M. Characterization of urethane-dimethacrylate derivatives as alternative monomers for the restorative composite matrix. *Dent. Mater.* **2014**, *30*, 1336–1344. [CrossRef]
40. Wan, J.; Li, C.; Bu, Z.-Y.; Xu, C.-J.; Li, B.-G.; Fan, H. A comparative study of epoxy resin cured with a linear diamine and a branched polyamine. *Chem. Eng. J.* **2012**, *188*, 160–172. [CrossRef]
41. Abd El-Fattah, M.; El Saeed, A.M.; Azzam, A.M.; Abdul-Raheim, A.-R.M.; Hefni, H.H. Improvement of corrosion resistance, antimicrobial activity, mechanical and chemical properties of epoxy coating by loading chitosan as a natural renewable resource. *Prog. Org. Coat.* **2016**, *101*, 288–296. [CrossRef]
42. Jouyandeh, M.; Shabanian, M.; Khaleghi, M.; Paran, S.M.R.; Ghiyasi, S.; Vahabi, H.; Formela, K.; Puglia, D.; Saeb, M.R. Acid-aided epoxy-amine curing reaction as reflected in epoxy/Fe_3O_4 nanocomposites: Chemistry, mechanism, and fracture behavior. *Prog. Org. Coat.* **2018**, *125*, 384–392. [CrossRef]
43. Jouyandeh, M.; Rahmati, N.; Movahedifar, E.; Hadavand, B.S.; Karami, Z.; Ghaffari, M.; Taheri, P.; Bakhshandeh, E.; Vahabi, H.; Ganjali, M.R. Properties of nano-Fe_3O_4 incorporated epoxy coatings from Cure Index perspective. *Prog. Org. Coat.* **2019**, *133*, 220–228. [CrossRef]
44. Parhizkar, N.; Shahrabi, T.; Ramezanzadeh, B. A new approach for enhancement of the corrosion protection properties andinterfacial adhesion bonds between the epoxy coating and steel substratethrough surface treatment by covalently modified amino functionalized graphene oxide film. *Corros. Sci.* **2017**, *123*, 55–75. [CrossRef]
45. Haasnoot, J.G. Mononuclear, oligonuclear and polynuclear metal coordination compounds with 1,2,4-triazole derivatives as ligands. *Coord. Chem. Rev.* **2000**, *200*, 131–185. [CrossRef]
46. Kumar, S.; Mukherjee, A.; Dutta, J. Chitosan based nanocomposite films and coatings: Emerging antimicrobial food packaging alternatives. *Trends Food Sci. Technol.* **2020**, *97*, 196–209. [CrossRef]
47. Davis, G.D.; Krebs, L.A.; Dacres, C.M. Coating evaluation and validation of accelerated test conditions using an in-situ corrosion sensor. *J. Coat. Technol.* **2002**, *74*, 69–74.
48. López-Ortega, A.; Bayón, R.; Arana, J.L. Evaluation of Protective Coatings for High-Corrosivity Category Atmospheres in Offshore Applications. *Materials* **2019**, *12*, 1325. [CrossRef] [PubMed]
49. Zhang, Z.X.; Liow, S.S.; Xue, K.; Zhang, X.; Li, Z.; Loh, X.J. Autonomous Chitosan-Based Self-Healing Hydrogel Formed through Noncovalent Interactions. *ACS Appl. Polym. Mater.* **2019**, *1*, 1769–1777. [CrossRef]